Small-angle x-ray scattering study of aqueous solutions of sulfonated calix[6]arene derivatives

Hideki Matsuoka, Mitsuyuki Tsurumi, and Norio Ise*
Department of Polymer Chemistry, Kyoto University, Kyoto 606, Japan
(Received 18 January 1988)

A small-angle x-ray scattering study has been carried out on aqueous solutions of three sulfonated calixarene derivatives (calix[6]arene-*p*-hexasulfonate (1-H), 5,11,17,23,29,35-hexasulfonato-37,38,39,40,41,42-hexakis-(hexyloxy)calix[6]arene (1-C_6), and 5,11,17,23,29,35-hexasulfonato-37,38,39,40,41,42-hexakis(dodecyloxy)calix[6]arene) (1-C_{12}). Except for 1-H, two distinct peaks were observed. The peak intensity at the lower angles became greater and the peak position shifted toward higher angles when the surfactant concentration was increased. This peak disappeared in high-salt conditions and was decreased in intensity with increasing temperature. These results were taken as implying that the peak reflects the intermicellar interference and that the micelles formed by the calixarene derivatives also form distorted ordered structures in solutions like many other ionic species studied earlier [N. Ise, Angew. Chem. **25**, 323 (1986)]. The intensity of the peak at larger angles became larger with increasing surfactant concentration but the peak position was not affected, indicating that this peak is due to intramicellar interference. From the observed intensity $I(Q)$ the intraparticle scattering function $[P(Q)]$ was estimated with the assumption that $I(Q)$ in high-salt conditions represents $P(Q)$. The $P(Q)$ thus obtained was compared with theoretical values computed for prolate ellipsoid core-shell models. The dimensions of the models were determined from the fitting. The aggregation number estimated from the models and the molecular size was found to be not very far from that obtained from the Bragg spacing.

It has been reported that the small-angle x-ray (SAXS) and neutron-scattering (SANS) curves for dilute solutions of ionic polymers such as proteins, polynucleotides, and synthetic macroions and of ionic aggregates such as ionic micelles show a single broad peak when the solute concentration is reasonably high, when the polymers are electrically charged, and when the coexisting salt concentration is sufficiently low.[1] We have taken the appearance of this peak as implying that the macroions are distributed in a more or less ordered manner even in dilute solutions. Unexpectedly, the intermacroion spacing calculated by the Bragg equation ($2D_{expt}$) has been found to be smaller than the average intermacroion distance ($2D_0$), which can be estimated from the concentration and the solution volume with the assumption of a uniform distribution of the macroions throughout the solution. The difference between the two spacings was particularly large for highly charged macroions and at low concentrations, the highest ratio observed being 1:3.5 for a high molecular weight polystyrene sulfonate.[2] From this observed fact it has been concluded that the ordered structure is localized and the so-called two-state structure is maintained; ordered regions of a high particle density coexist with less dense disordered regions.

In a recent theoretical consideration on the basis of a paracrystal theory, it has been affirmed that the intensity of scattered radiation from the cubic lattice systems with paracrystalline distortion is determined by the degree of the distortion, the thermal motion of the scattering elements (Debye-Waller effect), and the size of the lattice, but that the position of the scattering peaks is not affected by these three factors.[3] The theory has shown that higher-order peaks become indiscernible when the ordered structure of macroions is highly distorted. According to our interpretation, the single broad peak is therefore indicative of highly distorted ordered structures of the ionic species.

Our finding, that the macroions are arranged in an ordered manner in solutions and, furthermore, that the ordered structure is localized, has been so contradictory to commonly held beliefs that we were motivated to accumulate more direct experimental evidence in support of our interpretation: We initiated microscopic study of suspensions of ionic polymer latex particles, which are large enough to be observed under the ultramicroscope. The study has revealed almost unequivocally that these particles are also regularly distributed in suspensions at low-salt conditions. It has been confirmed that the interparticle spacing ($2D_{expt}$) directly estimated from the micrographs was smaller than the average interparticle spacing ($2D_0$) calculated from the concentration with the assumption of a uniform distribution for highly charged latices whereas $2D_{expt}$ was nearly equal to $2D_0$ for particles of a relatively low charge density.[1(b),4] When the inequality relationship, $2D_{expt} < 2D_0$, is satisfied, the two-state structure in latex suspensions has been confirmed by a photograph. According to recent computer-aided Fourier analysis of the micrographs (density function in real space), the ordered structure gave discrete spots in the Fourier patterns whereas the completely disordered structure provided neither spot nor ring. On the other hand, the Fourier pattern corresponding to the two-state

structure was intermediate between the two extremes, namely a few rather vague rings and spots.[5] This strongly supports our interpretation (in terms of translational ordering) of the single broad scattering peak observed for macroionic systems.

Some attempts were made to explain the origin of the SAXS peak by the so-called correlation-hole concept.[6] However, this concept, in which only a repulsive interaction between macroions is considered, cannot explain the molecular-weight dependence of the SAXS curve for synthetic ionic polymers. According to the correlation-hole concept, the scattering peak position is expected to be independent of the molecular weight of polyelectrolytes. However, a distinct molecular-weight dependence was observed for poly-L-lysine (PLL) (Ref. 7) and sodium polystyrene sulfonate (NaPSS).[2] This observation clearly indicates that the correlation-hole concept is not universally correct. Furthermore, the pH dependence of $2D_{expt}$ for bovine serum albumin (BSA),[8] i.e., a decrease of $2D_{expt}$ with increasing charge number of the BSA molecule, cannot be accounted for in terms of the repulsive interaction. If one accepts a repulsive interaction only, $2D_{expt}$ must become larger with increasing charge number. This is not experimentally the case, however. Therefore, one must take an attractive interaction between macroions into consideration in addition to the direct repulsive interaction. The attractive interaction is concluded to be an electrostatic one through the intermediary of counterions. For details, a recent convenient review should be consulted.[1]

Independently from this scattering study, an extended x-ray-absorption fine-structure (EXAFS) method has been applied to simple ionic solutions.[9] It has been concluded that even simple ions form an ordered arrangement in dilute solutions. It seems now that the ordering of ionic species in solution is quite general. Thus we thought it interesting to study further the scattering profiles of other ionic solutions. In the present paper we study water-soluble calixarene derivatives. As is clear from the chemical structure (see Fig. 1), they have fairly large numbers of ionized groups for low-molecular-weight compounds and may have varying degrees of hydrophobicity. We wanted to know the aggregation states of the calixarene derivatives, novel surface-active and/or clathrate compounds, in aqueous media, and their solution structure.

EXPERIMENTAL SECTION

The materials:

calix[6]arene-p-hexasulfonate (1-H),

5,11,17,23,29,35-hexasulfonato-37,38,39,40,41,42-hexakis-(hexyloxy)calix[6]arene (1-C_6),

and

5,11,17,23,29,35-hexasulfonato-37,38,39,40,41-42-hexakis(dodecyloxy)calix[6]arene (1-C_{12})

were synthesized by S. Shinkai, Nagasaki University.[10]

X-ray scattering experiments

The SAXS apparatus used was described in a previous paper,[2] except that a Ni filter is used in the present paper as a monochrometer. The measurements were done at room temperature (about 25 °C), except for the temperature-dependence measurements. The SAXS measurements of 1-C_6 were carried out at concentrations higher than the critical micelle concentration (CMC), which was reported to be $5.0\times10^{-4}M$ and $6.7\times10^{-4}M$ according to the surface tension and the conductivity measurements, respectively.[10] The CMC values for 1-H and 1-C_{12} were not found. The dissolution of 1-C_{12} was slow so the suspension was sonicated for several minutes until homogeneous solutions were obtained.

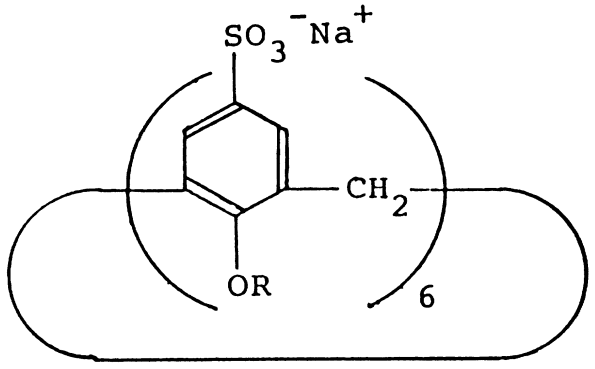

FIG. 1. Chemical structure of sulfonated calixarenes: 1-H (R = H), 1-C_6 (R = n-C_6H_{13}), 1-C_{12} (R = n-$C_{12}H_{25}$).

CALCULATION OF THE INTRAPARTICLE SCATTERING FUNCTION $P(Q)$ AND INTERPARTICLE SCATTERING FUNCTION $S(Q)$

For spherical micelles of ionic surfactant molecules, a core-shell model was proposed, in which the core and shell are composed of hydrophobic chains and hydrophilic parts, respectively. The intraparticle scattering function $P(Q)$ of this model can be written as follows:[11]

$$P(Q)=[\tfrac{4}{3}\pi R_{\rm par}^3(\rho_{\rm par}-\rho_{\rm pol})\Phi(R_{\rm par}Q) + \tfrac{4}{3}\pi R_{\rm pol}^3(\rho_{\rm pol}-\rho_0)\Phi(R_{\rm pol}Q)]^2 , \quad (1)$$

$$\Phi(u)=3[(\sin u - u\cos u)/u^3] , \quad (2)$$

where $R_{\rm par}$ and $R_{\rm pol}$ are the radii of the hydrophobic part and of the whole micelle, respectively; $\rho_{\rm par}$, $\rho_{\rm pol}$, and ρ_0 the electron densities of the hydrophobic part, the hydrophilic part, and the solvent, respectively; and Q (scattering vector) is $4\pi\sin\theta/\lambda$ with the wavelength λ and with the scattering angle 2θ. It is anticipated that the surfactant aggregates will grow from sphere to ellipsoid or cylinder, when the concentration increases. The general expression for the structure factor of a prolate ellipsoid model is given by[12,13]

$$P(Q)=\int_0^{\pi/2}\{V_{\rm pol}(\rho_{\rm pol}-\rho_0)\Phi[Q(\alpha+d)g_1(\theta)] + V_{\rm par}(\rho_{\rm par}-\rho_{\rm pol})\Phi[Q\alpha g_2(\theta)]\}^2\cos\theta\, d\theta , \quad (3)$$

where ρ_1, ρ_2, and ρ_0 are the electron density of the shell, core, and solvent, respectively, $V_{\rm pol}$ and $V_{\rm par}$ are the volumes of the whole particle and the core, respectively, d is the thickness of the shell, $g_1(\theta)=(\cos^2\theta+\nu'^2\sin^2\theta)^{1/2}$, $g_2\theta=(\cos^2\theta+\nu^2\sin^2\theta)^{1/2}$, and $\nu'=(\nu\alpha+d)/(\alpha+d)$ with the axial ratio ν (>1) and the axis length α. For a coated cylinder with outer diameter R, shell thickness d, and length $2H$, the structure factor is given by[12]

$$P(Q)=\int_0^{\pi/2}\left[V_{\rm pol}(\rho_{\rm pol}-\rho_0)\frac{\sin(QH\cos\theta)}{QH\cos\theta}\frac{2J_1(QR\sin\theta)}{QR\sin\theta} + V_{\rm par}(\rho_{\rm par}-\rho_{\rm pol})\frac{\sin(QH\cos\theta)}{QH\cos\theta}\frac{2J_1[Q(R-d)\sin\theta]}{Q(R-d)\sin\theta}\right]^2\sin\theta\, d\theta , \quad (4)$$

where J_1 denotes the first-order Bessel function.

The scattering intensity $I(Q)$ from interacting particles is generally written as[14]

$$I(Q)=n\{[\langle F^2(Q)\rangle-\langle F(Q)\rangle^2]+\langle F(Q)\rangle^2 S(Q)\} , \quad (5)$$

where $F(Q)$ is the scattering amplitude, $S(Q)$ the interparticle interference function, and n the number of particles per unit volume. In the case of anisotropic particles such as ellipsoids or cylinders, $\langle F^2(Q)\rangle=P(Q)$ and $\langle F^2(Q)\rangle\neq\langle F(Q)\rangle^2$. In the present work, the $P(Q)$ was determined by fitting the $P(Q)$ function to the observed intensity at high-salt conditions, where the interparticle contribution could be ignored, i.e., $S(Q)=1$. By using the set of parameters, which gave the best fit, $\langle F(Q)\rangle^2$ was calculated. The $S(Q)$ value was estimated from $I(Q)$ by using $P(Q)$ and $\langle F(Q)\rangle^2$ above determined together with the n values, which satisfied $P(Q)=I(Q)$ at higher scattering vectors.

RESULTS AND DISCUSSION

Concentration dependence of SAXS curves

Figures 2, 3, and 4 show the SAXS (relative) intensities of 1-H, 1-C_6, and 1-C_{12} at varying concentration as functions of the scattering vector (Q). Clearly the SAXS curves of 1-H did not show distinct Q dependence. This tendency is similar to that observed for surfactant solutions below the CMC. Thus it is suspected that 1-H does not form large aggregates such as micelles under the conditions employed, confirming the previous conclusion by Shinkai *et al.*[10] On the other hand, a sharp first peak and a broad second peak were observed for 1-C_6 (Fig. 3) and 1-C_{12} (Fig. 4). The first peak shifted toward higher angles with increasing surfactant concentration, while the intensity of the second peak was increased but its peak position was not influenced when the concentration was increased. The two peaks of 1-C_6 are located at higher angles than those of 1-C_{12}. It is to be noted that the Bragg spacing ($2D_{\rm expt}$) for 1-C_6 calculated from the first peak was about 100 Å, whereas that of 1-C_{12} was in the range between 200 and 400 Å. For both the surfactants, the $2D_{\rm expt}$ value decreased with increasing concentration. This concentration dependence is in accord with that found for other ionic surfactants and various macroions,[1,2] indicating that the first peak is due to intermicellar interference. On the other hand, the position of the second peak did not change with concentration as mentioned above, and furthermore does not correspond to the second-order diffraction peak of common crystal systems such as fcc, bcc, etc. Thus the second peak is considered

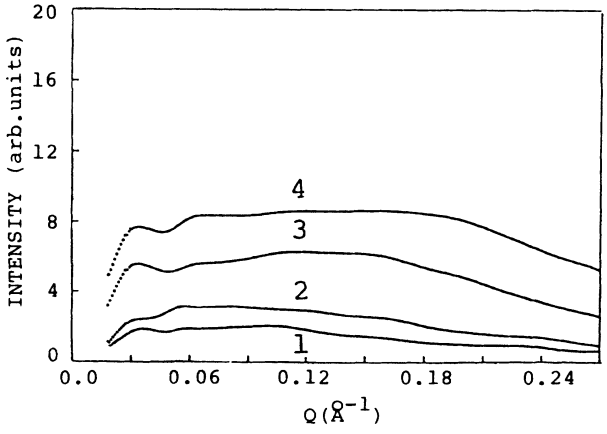

FIG. 2. Influence of the concentration on the scattering curves of 1-H: 1, 0.008 g/ml; 2, 0.016 g/ml; 3, 0.04 g/ml; 4, 0.08 g/ml.

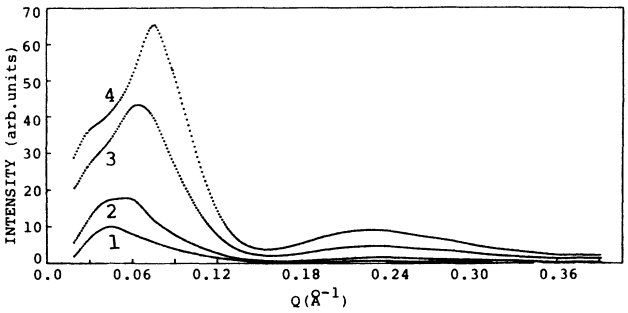

FIG. 3. Influence of the concentration on the scattering curves of 1-C_6: 1, 0.008 g/ml; 2, 0.016 g/ml; 3, 0.04 g/ml; 4, 0.08 g/ml.

to be due not to interparticle interference but to intraparticle scattering. Although the graphical presentation has been omitted, the intensities of the second peaks of 1-C_6 and 1-C_{12} are represented by a straight line passing through the origin in the intensity-concentration plot. Furthermore, $I(Q)/C$ curves [the scattering intensity normalized for the concentration (C)] shows an excellent agreement for the shape of the second peak. These facts suggest that the second peak reflects the shape of the particles, which is believed to be practically constant over the concentration range employed.

Tables I and II show the relevant SAXS data of 1-C_6 and 1-C_{12}, in which I_{max} is the relative intensity at the peak position, Q_m the scattering vector at the peak, $2D_{expt}$ the interparticle distance calculated from Q_m, and $\bar{n}$ the aggregation number of the surfactant in one micelle. The $\bar{n}$ value was calculated by assuming that $2D_{expt}$ is equal to $2D_0$, which can be estimated on the assumption that the micelles are uniformly distributed throughout the solution in a simple-cubic lattice. The assumption, $2D_{expt}=2D_0$, has always been satisfied for ionic entities of low charge density[2] such as ionic micelles.[15]

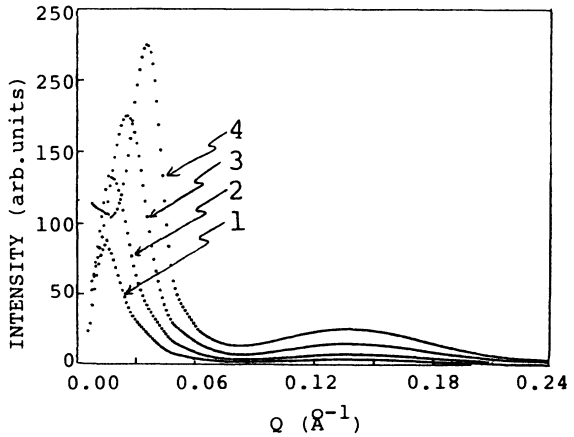

FIG. 4. Influence of the concentration on the scattering curves of 1-C_{12}: 1, 0.01 g/ml; 2, 0.02 g/ml; 3, 0.04 g/ml; 4, 0.08 g/ml.

TABLE I. SAXS data of 1-C_6 in aqueous solutions.

Conc. (g/ml)	I_{max} (counts/sec)	Q_m (Å^{-1})	$2D_{expt}$ (Å)	$\bar{n}$ [a]
0.008	10.2	0.046	138	7
0.016	18.1	0.055	115	8
0.04	43.5	0.064	97	13
0.08	65.4	0.076	82	15

[a]Aggregation numbers calculated from $2D_{expt}$.

The $\bar{n}$ value obtained for 1-C_6 is close to that reported by Shinkai *et al.*[10] and the agreement is more satisfactory at low concentrations. Furthermore, the $\bar{n}$ value increased with increasing concentration of 1-C_6. The critical point in the above argument is naturally the validity of the assumption that $2D_{expt}=2D_0$. If 1-C_6 forms much more highly charged micelles, this assumption fails and we should expect $2D_{expt}<2D_0$, as has been observed for highly charged ionic species.[2] If this is really the case for 1-C_6, larger $\bar{n}$ values must result. Further, the difference between $2D_{expt}$ and $2D_0$ should become smaller with increasing concentration, as has been observed[2] and will be easily accepted. Then the $\bar{n}$ value at lower concentrations would be larger. Contrarily, the model calculation to be described below appears to justify, though roughly, the $\bar{n}$ value given in Table I. Another point is that $2D_{expt}$ in Table I was calculated from $I(Q)$; to be exact, it should have been estimated from $S(Q)$. The $S(Q)$ of 1-C_6 could not be estimated but its peak position must be at higher Q values than $I(Q)$ as has been observed,[15] since the $P(Q)$ decreases monotonically with increasing Q in the Q range where the first peak was observed. If this is the case, $2D_{expt}$ from $S(Q)$ would be smaller than that from $I(Q)$ (given in Table I), resulting in smaller values. Anyway, the quantitative aspect of the magnitude of the $\bar{n}$ value remains unsolved, and must be considered in the future.

The above argument about $\bar{n}$ would apply also for 1-C_{12}. It is to be noted that the geometrical model to be considered below indicates a higher charge density for 1-C_{12} than for 1-C_6. If so, $2D_{expt}<2D_0$ might be expected to hold, and then a larger $\bar{n}$ value would result. Although we will discuss again this parameter of 1-C_{12} in connection with its $S(Q)$ below, it is pointed out that our results are at variance with those of Shinkai *et al.*,[10] who concluded that 1-C_{12} exists as an oligomer. One factor could be the concentration difference; their concentrations are below $\frac{1}{10}$ of ours.

Salt-concentration dependence of SAXS curves

Figures 5 and 6 show the SAXS curves in the presence of added NaCl. In its absence, both 1-C_6 and 1-C_{12} had two peaks (Figs. 3 and 4). The first peak disappeared at high-salt conditions, as was observed for other ionic polymer systems.[1(b)] This suggests that the ordered structure

TABLE II. SAXS data of 1-C_{12} in aqueous solutions.

Conc. (g/ml)	I_{max} (counts/sec)	Q_m (Å^{-1})	$2D_{expt}$ (Å)	$\bar{n}$ [a] from $I(Q)$	$\bar{n}$ [a] from $S(Q)$
0.01	87.94	0.016	390	158	158
0.02	131.4	0.018	344	217	124
0.04	175.7	0.026	244	154	87
0.08	224.6	0.034	183	130	84

[a]Aggregation numbers calculated from $2D_{expt}$.

is due to electrostatic interaction. On the other hand, the second peak was not as much influenced by the salt addition as the first one, but the second peak for 1-C_6 was more influenced. The insensitivity of the second peak toward the salt addition confirms that this peak reflects the intraparticle scattering. The slightly larger influence on 1-C_6 would be due to its smaller aggregation number; a change in the aggregation number caused by the added salt would result in a relatively larger change in smaller micelles than in larger ones. It is expected that the aggregation number would increase with increasing salt concentration, as was the case for conventional surfactants.

Temperature dependence of SAXS curves

Temperature dependence of the SAXS curves for 1-C_{12} is demonstrated in Fig. 7. Table III shows the relevant SAXS data. When the temperature was raised, the position of the first peak was seen to shift toward higher angles, though slightly, and its peak height was lowered. The second peak was not affected.

The change of the first peak is consistent with that observed for linear macroions.[2] The decrease in the intensity would indicate the thermally enhanced distortion of the ordered structure. The position shift, though small, would be due to the decrease in the aggregation number, which would be caused by the lowering in the dielectric constant of water (with increasing temperature) and hence the enhanced short-range electrostatic (repulsive) interaction between the ionic charges of the surfactant molecules.[16] As a matter of fact, the $\bar{n}$ value in Table III, which was calculated on the assumption that $2D_{expt}=2D_0$, decreases with temperature. Another factor to be considered might be that the micelles become less stable at higher temperature. Furthermore, the shift of the peak position toward higher Q values with temperature might be a consequence of intensification of the medium-range attractive intermicellar interaction, which determines the position of the secondary minimum in the potential curve together with the short-range repulsive interaction. However, it seems to us premature to conclude something definite on the temperature dependence of $\bar{n}$, since assumption, $2D_{expt}=2D_0$, has not been finally warranted for the present systems, since the $2D_{expt}$ was estimated from $I(Q)$, not from $S(Q)$, and since information about the packing state of the surfactant molecules in the micelles is lacking.

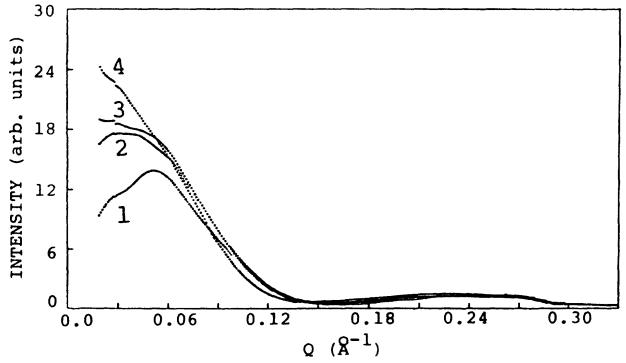

FIG. 5. Influence of the NaCl concentration on the scattering curves of 1-C_6. The 1-C_6 concentration is 0.016 g/ml. The NaCl concentration is shown with the following curves: 1, 0.00M; 2, $2.5\times10^{-2}M$; 3, $5.0\times10^{-2}M$; 4, $1.0\times10^{-1}M$.

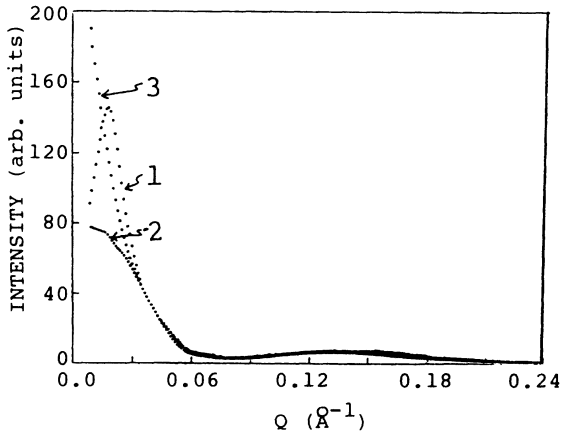

FIG. 6. Influence of the NaCl concentration on the scattering curves of 1-C_{12}. The 1-C_{12} concentration is 0.02 g/ml. The NaCl concentration is shown with the following curves: 1, 0.00M; 2, 0.01M; 3, 0.05M.

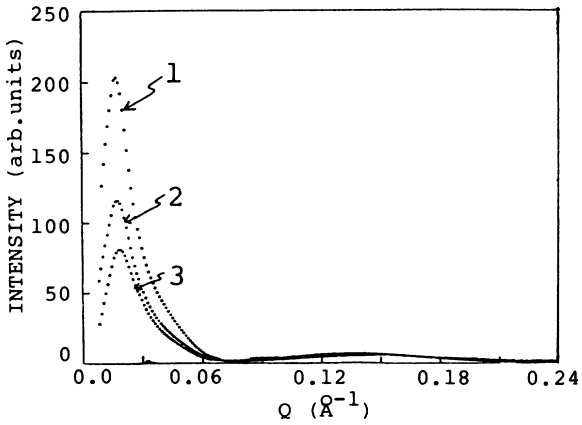

FIG. 7. Temperature dependence of scattering curves for 1-C_{12}. The 1-C_{12} concentration is 0.02 g/ml. The curves are as follows: 1, 12 °C; 2, 25 °C, 3, 41 °C.

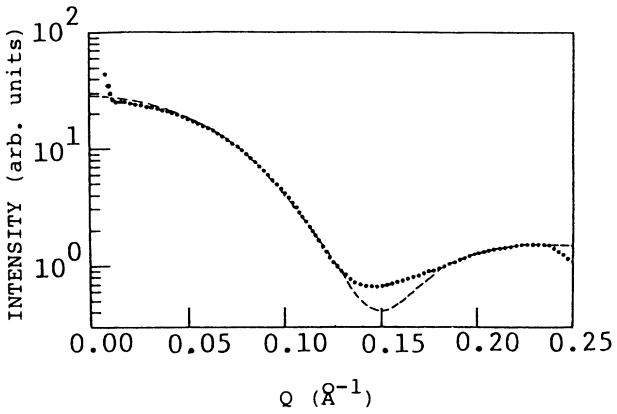

FIG. 8. Fitting of the experimental SAXS curves of 1-C_6 with the intraparticle scattering factor of a prolate ellipsoid. ●, experimental curves: [1-C_6]=0.016 g/ml and [NaCl]=0.10M. — — —, theoretical curve: R =5.0 Å, ν=3.7, and d=16.0 Å, ρ_{par}=0.229 electrons/Å^3, ρ_{pol}=0.351 electrons/Å^3, ρ_0=0.334 electrons/Å^3.

Computation of $P(Q)$ and model fitting

1-C_6

The scattering intensity observed at high-salt conditions is expected to provide the intraparticle scattering function $P(Q)$. In this section $P(Q)$ was computed with a prolate ellipsoid core-shell model. This model was chosen because it can fit the actual micelles by adjusting the parameters involved even if they assume the shapes of cylinders, spheres, or disks. Figure 8 is the result of the computation and the comparison with the experimental curve for 1-C_6. In this figure, the dashed curve is the computed one whereas the dotted curve is experimental and the ordinate gives the relative intensity in a logarithmic scale to facilitate comparison with the computation. For ρ_{par}, the average electron density estimated for n-hexane was used. The average electron density of an aqueous NaCl solution of 0.10M was used for ρ_0. By the trial and error method, other parameters were determined to give the best fit with the observed intensity. As is seen from Fig. 8, the agreement is fairly satisfactory: The disagreement at Q =0.15 was not so striking in the nonlogarithmic scale. Using the parameter values thus determined, the ellipsoid is reproduced in Fig. 9, in which two cross sections are demonstrated. The dark area corresponds to the space occupied by the hydrophobic carbon chains, whereas the less dark area is occupied by oxygen, benzene ring, methylene, and sulfonate groups, counterions and their hydrating water. We note that the parameter values found agreed satisfactorily with the ones from the Corey-Pauling-Koltun (CPK) model, except that the thickness of the shell was larger than the CPK value because the distance of the dissociated counterions from the sulfonate group was not known. According to the CPK model, the micelle is judged to be nearly spherical when $\bar{n}$ is 6. Further increase in the $\bar{n}$ is supposed to cause a nonspherical shape. According to a simple estimation, the core part can accommodate 6–12 surfactant molecules whereas the total volume corresponds to 10–20 molecules. Since the number of surfactant molecules must be the same in the shell and core parts, the packing in the shell part is expected to be less dense and the largest aggregation number must be smaller than 12. This value is fairly close to that in Table I, which was obtained from the assumption that $2D_{expt}=2D_0$.

We tried also to compute $S(Q)$ from $I(Q)$. Because of the comparatively large variation of the observed intensity with salt concentration, this was not successful.

1-C_{12}

In Fig. 10, the theoretical curve of $P(Q)$ for 1-C_{12} based on a prolate ellipsoidal core-shell model (dashed

TABLE III. Temperature dependence of SAXS data of 1-C_{12}.

Conc. (g/ml)	Temp. (°C)	I_{max} (counts/sec)	Q_m (Å^{-1})	$2D_{expt}$ (Å)	$\bar{n}$ [a]
0.02	12	203.3	0.017	365	260
	25	116.0	0.018	344	217
	41	81.4	0.019	324	183

[a]Aggregation numbers calculated from $2D_{expt}$.

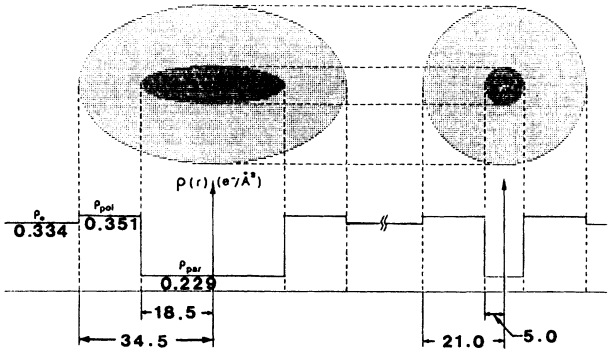

FIG. 9. Model for ellipsoid micelle of 1-C_6.

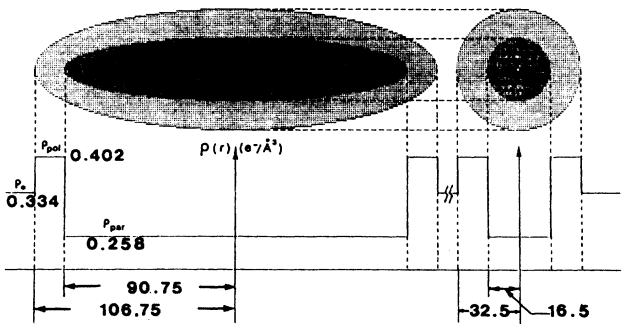

FIG. 11. Model for ellipsoid micelle of 1-C_{12}.

curve) is compared with the observed one (solid circles). The calculated intensity for a coated-cylinder model was also shown (dash-dotted curve) for comparison. The ρ_{par} used was the average electron density calculated from the average density of *n*-dodecane and the ρ_0 was the electron density of 0.05*M* NaCl solution. The thickness of the shell, *d*, was the same as that used for 1-C_6. The agreement between the computation for the ellipsoid and experiment is satisfactory except at $Q=0.08$. As we mentioned already for 1-C_6, the disagreement is not so serious in the linear plot. The core radius and the shell thickness used in the computation were in good agreement with the values expected from the CPK model. Since the ν value used in the fitting by the ellipsoid model was fairly large ($\nu=5.5$), we tried fitting with a coated-cylinder model. However, the agreement with experiment was less satisfactory, especially for the minimum at $Q=0.08$ and for the higher-angle region ($Q>0.15$), as easily seen from Fig. 10, although the gratifying agreements of the scattering behavior in the small-angle region ($Q<0.06$) and the height and the position of the second maximum were obtained with a slightly larger ρ_{pol} value (0.442) and with a shorter length ($H=90.0$ Å) than those used for the ellipsoid model. By using the size parameter values estimated by the above fitting, the ellipsoid is drawn and shown in Fig. 11. It is believed that, in the middle portion of the ellipsoid, 8–10 surfactant molecules form a disk and several disks stick together to form the ellipsoid. The aggregation state at both the ends of the ellipsoid is not clear but it is believed that the cross section of the ellipsoid is covered by hemispheres with the hydrophilic part of 1-C_{12} outward. The $\bar{n}$ value expected from the core volume and the total volume is roughly 130, suggesting that the 1-C_{12} micelle is more densely packed than the 1-C_6 micelle. As a matter of fact, the electron density value of 1-C_{12} (0.402) used for the computation is higher than that for 1-C_6 (0.351).

Since the scattering curves of 1-C_{12} were not sensitive to the salt concentration, the $S(Q)$ function was calculated by using Eq. (5) with the assumption that the micelle

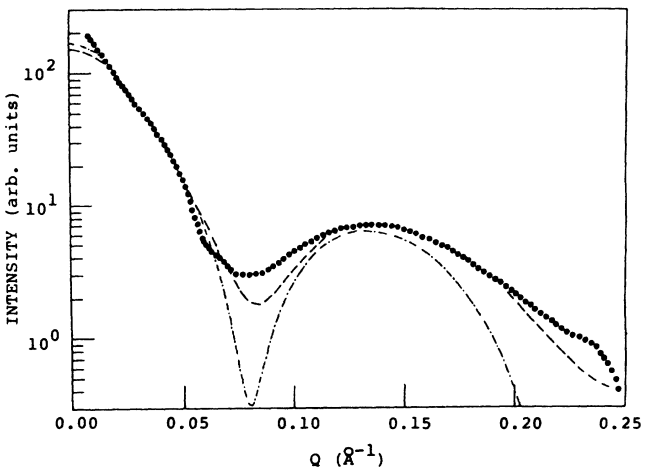

FIG. 10. Fitting of the experimental SAXS curve of 1-C_{12} with the intraparticle scattering factors of a prolate ellipsoid and of a coated cylinder. ●, experimental curve: [1-C_{12}]=0.02 g/ml and [NaCl]=0.05*M*. — — —, theoretical curve: $R=16.5$ Å, $\nu=5.5$, $d=16.0$ Å, $\rho_{par}=0.258$ electrons/Å^3, $\rho_{pol}=0.402$ electrons/Å^3, $\rho_0=0.334$ electrons/Å^3. —·—·—·, theoretical curve for cylinder: $R=32.5$ Å, $d=16.0$ Å, $H=90.0$ Å, $\rho_{par}=0.258$ electrons/Å^3, $\rho_{pol}=0.442$ electrons/Å^3, $\rho_0=0.334$ electrons/Å^3.

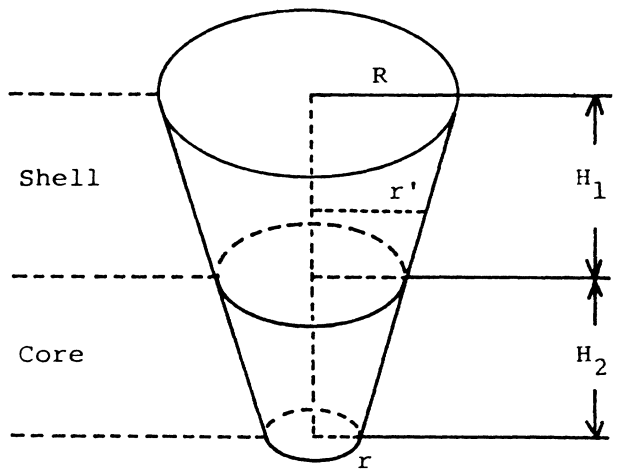

FIG. 12. Highly simplified molecular model of 1-C_6 and 1-C_{12}.

size and shape did not change with salt concentration. The $S(Q)$ function is supposed to give more reliable information on the intermicellar spacing of $2D_{expt}$ than $I(Q)$. The $2D_{expt}$ values thus obtained are given in Table II. The spacing from $S(Q)$ is generally smaller, though slightly, than that from $I(Q)$, as was observed earlier.[15] Furthermore the $\bar{n}$ value was calculated from $S(Q)$ by assuming $2D_{expt}=2D_0$, and is shown in Table II. However, it seems to us that the $\bar{n}$ value, particularly that from $S(Q)$, should be viewed with caution, because it was estimated by assuming the constant size and shape and, nevertheless, the $\bar{n}$ value obtained changed with concentration. Furthermore, the other assumption, $2D_{expt}=2D_0$, in the calculation would be less reliable for 1-C_{12} than for 1-C_6, since the aggregate of the former deviates substantially from a sphere, for which only $2D_{expt}$ can be significantly compared with $2D_0$. As far as the $\bar{n}$ value is concerned, we should be satisfied with the rough agreement between the value from $I(Q)$ and that from the ellipsoidal model (about 150).

Estimation of the aggregation number ($\bar{n}$)

The $\bar{n}$ of the surfactants was determined from the volume of the single molecule (v) and the volume of the micelle (V). v was calculated by using the interatomic distances: 1.52 Å for C—C, 1.40 Å for C=C (benzene ring), 1.11 Å for C—H, 1.42 Å for C—O, 1.78 Å for C—S, and 1.43 Å for S=O. The bond angles assumed were 112° for ∠C—C—C, 112° for ∠C—O—C, 105.7° for ∠C—S—O, and 108° for ∠H—C—H. The ionic radius assumed for Na^+ was 1.16 Å. By using these data, the fully stretched n-alkane chain was found to be 7.2–8.38 Å long for 1-C_6, depending on whether or not the oxygen atom is included. The corresponding length for 1-C_{12} was 14.76–15.94 Å. The distance between the oxygen adjacent to the alkyl chain and the Na^+ was 10.4 Å. The radius of a circle formed by the benzene rings and the methylene groups (r') was about 5.4 Å.

The alkane chain length mentioned above appears to be consistent with the core radius (5 Å) of the model (Fig. 9) constructed on the basis of the x-ray analysis. The smaller value deduced from the x-ray measurement would be acceptable, since the aggregation number of this surfactant (and hence the packing density) is rather small so that bending of the carbon chain inside the core would be more feasible than in the case of 1-C_{12}.

For simplicity, the surfactant molecules were assumed to have the shape shown in Fig. 12. The truncated cone with the height H_1 represents the shell, in which the hydrophilic part of the micelle is accommodated. The rest, with the height H_2, correspond to the hydrophobic part. H_1 and H_2 were assumed to be equal to the thickness of the shell and the core radius in Figs. 9 and 11, respectively: $H_1=16$ Å, $H_2=5$ Å for 1-C_6 and $H_1=16$ Å, $H_2=16.5$ Å for 1-C_{12}. For the r value, 3.3 Å was assumed for 1-C_6 and 1-C_{12}.

By dividing V with v, the aggregation number ($\bar{n}$) was deduced. For 1-C_6, V was 63 730 Å^3 and $\bar{n}$ was found to be 20, 17, and 15 for $R=10$, 11, and 12 Å, respectively. The assumed R values may be justified, though not highly convincingly, since R must be equal to or larger than r' (5.4 Å). For 1-C_{12}, V was 472 310 Å^3 and $\bar{n}$ was estimated to be 208, 167, and 137 for $R=6$, 7, and 8 Å, respectively. The difference in the R values for the two surfactants reflects the higher packing density of 1-C_{12}. It should be pointed out that, if the dead space between the molecules is taken into consideration, the $\bar{n}$ values thus obtained are roughly of the same order of magnitude as those estimated from the scattering peak position (and hence the intermicellar distance, $2D_{expt}$) shown in Tables I and II.

ACKNOWLEDGMENTS

Valuable comments were obtained from Professor G. Hall. The materials used were kindly donated by Professor S. Shinkai. He also furnished basic data on the surfactants. This work was supported by a grant-in-aid for specially promoted research administered by the Ministry of Education, Science, and Culture.

*To whom correspondence should be addressed.

[1]For convenient reviews of this topic, see (a) N. Ise and T. Okubo, Acc. Chem. Res. **13**, 303 (1980); (b) N. Ise, Angew. Chem. **25**, 323 (1986).

[2]N. Ise, T. Okubo, S. Kunugi, H. Matsuoka, K. Yamamoto, and Y. Ishii, J. Chem. Phys. **81**, 3294 (1984).

[3](a) D. J. Yarusso and S. L. Cooper, Macromolecules **16**, 1871 (1983); (b) H. Matsuoka, H. Tanaka, T. Hashimoto, and N. Ise, Phys. Rev. B **36**, 1754 (1987).

[4]K. Ito, H. Nakamura, and N. Ise, J. Chem. Phys. **85**, 6136 (1986).

[5]K. Ito and N. Ise, J. Chem. Phys. **86**, 6502 (1987).

[6]J. B. Hayter, G. Jannink, F. Brochard-Wyart, and P. G. de Gennes, J. Phys. (Paris) **41**, L-451 (1980).

[7]N. Ise, T. Okubo, K. Yamamoto, H. Matsuoka, H. Kawai, T. Hashimoto, and M. Fujimura, J. Chem. Phys. **78**, 541 (1983).

[8]H. Matsuoka, N. Ise, T. Okubo, S. Kunugi, H. Tomiyama, and Y. Yoshikawa, J. Chem. Phys. **83**, 378 (1985).

[9]A. Sadoc, A. Fontaine, P. Lagarde, and D. Raoux, J. Am. Chem. Soc. **103**, 6287 (1981).

[10]S. Shinkai, S. Mori, H. Koreishi, T. Tsubaki, and O. Manabe, J. Am. Chem. Soc. **108**, 2409 (1986).

[11]R. Friman and J. B. Rosenholm, Colloid Polym. Sci. **260**, 545 (1982).

[12]S. H. Chen, M. Holtz, and P. Tartaglia, Appl. Opt. **16**, 187 (1977).

[13]J. Marignan, P. Basserau, and P. Delord, J. Phys. Chem. **90**, 645 (1986).

[14]J. B. Hayter and J. Penfold, Colloid Polym. Sci. **261**, 1022 (1983).

[15]Y. Ishii, H. Matsuoka, and N. Ise, Ber. Bunsenges. Phys. Chem. **90**, 50 (1986).

[16]In light of the insensitivity of the second peak toward temperature, the change of the $\bar{n}$ value with temperature would not be as large as shown in Table III.

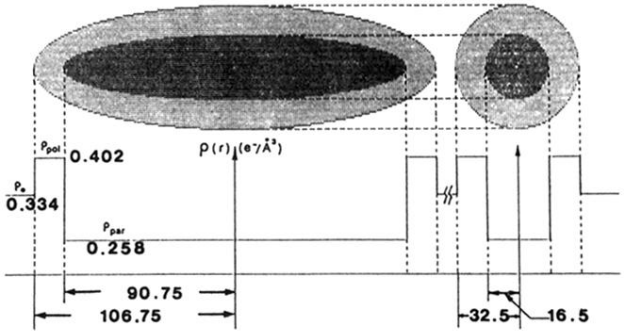

FIG. 11. Model for ellipsoid micelle of 1-C_{12}.

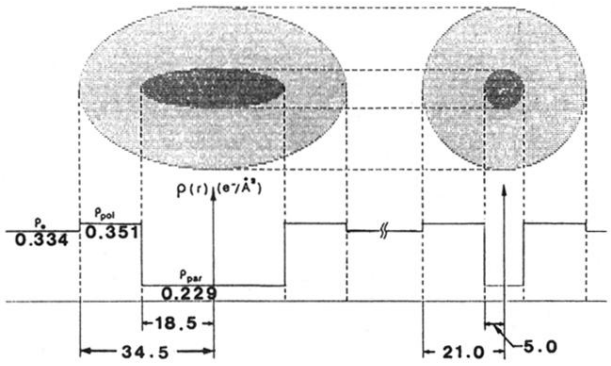

FIG. 9. Model for ellipsoid micelle of 1-C_6.